IEEE Access
Multidisciplinary ⋮ Rapid Review ⋮ Open Access Journal

Received 20 September 2023, accepted 17 October 2023, date of publication 25 October 2023, date of current version 1 November 2023.

Digital Object Identifier 10.1109/ACCESS.2023.3327525

RESEARCH ARTICLE

Brushless Wound Rotor Synchronous Machine Topology Using Concentrated Winding for Dual Speed Applications

SHEERAZ AHMED[1], MUDASSIR RAZA SIDDIQI[2], QASIM ALI[1], TANVEER YAZDAN[3], ASIF HUSSAIN[4], AND JIN HUR[2], (Fellow, IEEE)

[1]Department of Electrical Engineering, Sukkur IBA University, Sukkur 65290, Pakistan
[2]Electrical Engineering Department, Incheon National University, Incheon 22012, South Korea
[3]Electrical Engineering Department, The University of Lahore, Lahore 54000, Pakistan
[4]Department of Electrical Engineering, University of Management and Technology, Lahore 54770, Pakistan

Corresponding author: Jin Hur (jinhur@inu.ac.kr)

This work was supported by the Industrial Strategic Technology Development Program of Korea Planning and Evaluation Institute of Industrial Technology (KEIT) under Grant 20023790 and Grant 20018442.

ABSTRACT Permanent magnet (PM) machines have broad applicability and a rapid output rise due to their good power factor, high efficiency, and power density. However, with the recent high cost, unavailability, and demagnetization issues of PMs, the wound rotor synchronous machine (WRSM) is a better substitute for permanent magnet machines for various applications in terms of price value and controllability. While the WRSM contains issues such as regular maintenance and replacement of brushes and slip rings, this paper introduces a brushless WRSM (BL-WRSM)with concentrated winding having 36 slots and 48 poles, which generates fundamental component and a dominant sub-harmonic component of magneto motive force (MMF). To achieve the brushless operation, the rotor has an additional winding called excitation winding that is connected with the main field winding via a rectifier. This additional winding is used to induce the electromotive force (EMF) by the sub-harmonic MMF component of the stator. The EMF is converted to DC by the rectifier and fed to the main field winding. This BL-WRSM has been developed for dual-speed applications such as washing machines. The machine has been tested for 46 rpm and 1370 rpm. The low-speed mode is for washing and the high-speed mode is for drying clothes. To validate the performance and feasibility, an outer rotor BL-WRSM is designed. The performance was compared with the conventional WRSM (C-WRSM). 2-D finite element analysis (FEA) simulation was conducted using ANSYS Electromagnetic.

INDEX TERMS Brushless operation, brushless excitation, finite element analysis (FEA), outer rotor wound rotor synchronous machine, dual speed operation.

I. INTRODUCTION

The role of electrical energy in our daily lives is immense, and it has become a very important part of our lifestyle. It is difficult to imagine a world without electricity, as almost every aspect of our lives depends on it. The importance of electricity in modern-day living can be understood by measuring the standard of living based on the average amount of energy consumed by residents, in commercial and industrial zones.

Electric machines play a crucial role in the generation, transmission, and utilization of the generated energy. Two major types of electric machines, permanent magnet (PM) machines, and induction machines dominate the industry. PM machines are mostly preferred due to their high power density, high efficiency, and high performance in various applications. In contrast, induction machines are known for their ruggedness, dependability, and low maintenance.

The associate editor coordinating the review of this manuscript and approving it for publication was Giambattista Gruosso.

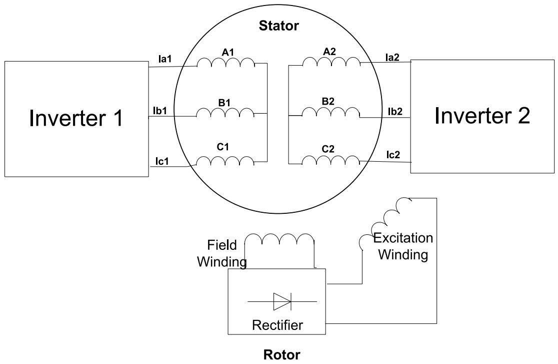

FIGURE 1. BL-WRSM with dual inverter topology.

However, the availability of PM materials such as Neodymium iron boron (NdFeB) is becoming increasingly scarce and expensive. Recent reports have shown that permanent magnet material availability will decline as companies shut down their manufacturing facilities for permanent magnets [1]. Researchers are finding new and alternative ways to make existing machine topologies more efficient, and one such way is to convert a brushed machine into a brushless one.

A. BRUSHLESS WOUND ROTOR MACHINES

A Wound Rotor Synchronous Machine (WRSM) is a type of electric machine that has winding on the rotor called the field windings. The slip rings and brushes are used to deliver power to the rotor main field windings.WRSMs have several advantages over other types of electric machines. One of the most significant advantages of WRSMs is that they do not require costly permanent magnets. This reduces the overall cost of the machine and makes it more affordable for various applications. Additionally, WRSMs offer variable speeds and the ability to modify rotor excitation current, resulting in better efficiency under low load conditions for variable speed operations without flux weakening.

Although WRSMs offer several advantages over other types of electric machines, they also have some challenges and limitations. One of the significant challenges is the use of slip rings and brushes to deliver power to the rotor windings. The use of brushes and slip-rings leads to regular maintenance, power loss, and reduction in efficiency.

In recent years, some topologies have emerged for the brushless WRSM (BL-WRSM). A new topology was presented in [2] using the harmonic operation and sub-harmonic method. Fig. 1 shows the topology introduced by [2]. Two inverters were used to excite the stator's distributed winding. The difference in amplitude of the currents provided by both inverters generated the sub-harmonic component. Based on the topology of [2], multiple designs were introduced in [3], [4], and [5]. In [3], the winding configuration was altered to improve efficiency. In [4] the 8-pole model was designed to overcome the problems associated with the 4-pole design. In [5], a Pm-assisted model was introduced which improves the developed torque of the machine.

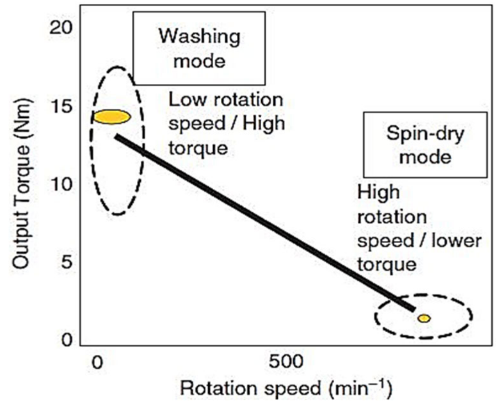

FIGURE 2. Requirements of washing machine's motor [15].

To overcome the cost issues of dual inverter topology, different single inverter topologies which were also based upon sub-harmonic BL-WRSM were introduced in [6], [7], [8], and [9]. In [6] the machine has been developed for conventional WRSM and BL-WRSM. In [7], the sub-harmonic is produced by changing the number of turns in half of the slots of stator winding. In [8], symmetrical stator winding distribution was introduced for sub-harmonic BL-WRSM. In [9], the single inverter brushless topology has been extended to the Vernier machine.

In [10] dual mode BL-WRSM has been introduced in which, the machine works in induction mode and synchronous mode.

In [11] and [12], higher harmonic components of the stator MMF are utilized for the BL-WRSM. Both of these topologies utilize the third harmonic component of the stator MMF for brushless excitation purposes. Higher harmonic topologies have been less utilized due to the concern of higher losses compared to sub-harmonic topologies.

Until now, all the work done in the field of brushless excitation requires either multiple inverters, switches or special winding configurations to generate the harmonic component in the stator MMF.

B. DUAL SPEED DIRECT DRIVE HOME APPLICATIONS

The worldwide market of home appliances is growing steadily, principally in Latin America, China, Africa, Eastern Europe, Southeast Asia, and the Middle East. Washing machines are undoubtedly the most important home appliances, used by billions of customers worldwide [13]. They have had continuous and consistent technology development while reducing energy consumption. The smart appliance market generated revenue of 28.5 billion U.S. dollars worldwide in 2020 and the Statista Digital Market Outlook estimates that by 2025 this market will grow to 67.6 billion dollars in revenue [14].

Washing machine operation is characterized broadly into two main cycles: Wash Cycle and Spin Dry Cycle. During the washing cycle, laundry is tumbled to create an effective washing at around 50 to 60 rpm of drum speed. During the spin dry cycle, the remaining water is extracted from

-A	-C	-B	-A	-C	-B	-A	-C	-B	-A	-C	-B	-A	-C	-B	-A	-C	-B	-A	-C	-B	-A	-C	-B	-A	-C	-B	-A	-C	-B	-A	-C	-B	-A	-C	-B
C	B	A	C	B	A	C	B	A	C	B	A	C	B	A	C	B	A	C	B	A	C	B	A	C	B	A	C	B	A	C	B	A	C	B	A

FIGURE 3. Stator winding arrangement.

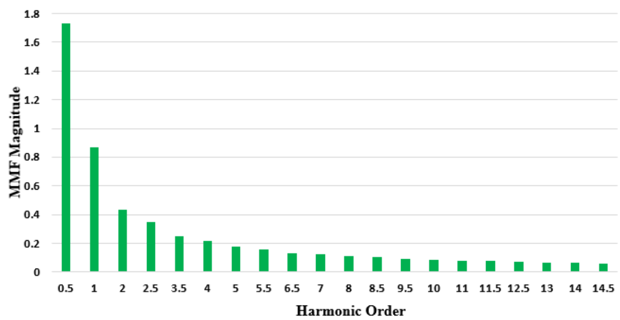

FIGURE 4. Harmonic components of MMF FFT analysis.

the laundry by making use of centrifugal forces by running the drum at very high speeds of 800 to 1600 rpm [15]. The torque requirements also change during both cycles, a torque of 15-20 Nm is required in the wash cycle and around 3-5 Nm in the dry cycle.

Switched reluctance motors (SRM) for washing machine applications have been discussed in [16], [17], and [18]. In [16] reconfigurable winding topology has been proposed to enhance the efficiency of the motor. In [17], T-Type Stator Pole for stator has been introduced for performance improvement. In [18], 2phase SRM for Bidirectional Starting has been introduced. Apart from SRM, a Dual-Mechanical-Port Dual-Excitation Machine based upon PM Vernier and PM synchronous motor (PMSM) has been introduced.

In this paper, to reduce the costs of PMs as well as achieve high torque and noiseless operation which is a major concern in SRM, a new BL-WRSM has been introduced. A simplified solution for the brushless excitation is proposed by introducing the concentrated winding in the stator. The pole slot combination chosen for the proposed machine inherently possesses the sub-harmonic component that is required for the rotor excitation.

In the next section, the proposed configuration of the machine is discussed in detail. After that, the 2-D FEA results and comparison with C-WRSM are drawn. Finally, the conclusion is presented.

II. PROPOSED BRUSHLESS TOPOLOGY

In this paper, a new winding topology has been used. The stator has three-phase winding placed in 36 slots with 48 poles. The winding is double layered with a coil span of 1 slot. The winding configuration of the proposed machine is shown in Fig. 3.

The MMF generated by this winding arrangement in the airgap has two dominant components i-e the fundamental component which has a harmonic order of 1 and the sub-harmonic component which has a harmonic order of 0.5 as shown in Fig. 4.

Previously, some research has been carried out to reduce the subharmonic and higher harmonic components in the MMF of fractional slot concentrated winding in AC machines [20], [21].

As was seen in other brushless topologies [2], [3], [4], [5], [6], [7], [8], [9], [10], [11], [12], some special circuitry or stator winding topology was employed to achieve the brushless operation, which needs additional space and cost.

But the proposed machine with 36 slots and 48 poles, having concentrated winding, is chosen to utilize the sub-harmonic component generated in its stator MMF. The proposed machine does not need any additional inverter or stator winding for the sub-harmonic generation it utilizes the inherently developed sub-harmonic generated by the winding arrangement employed.

The electric loading A is defined as linear current density around the air-gap circumference or the number of ampere-turns around the air-gap and can be mathematically expressed as per (1):

$$A = \left(2^{*}m^{*}N_{PH}{}^{*}I\right) / \left(\pi^{*}D_{AIR}\right) \tag{1}$$

where N_{PH} is the number of phase turns, m is the number of phases, D_{AIR} is the air-gap diameter, and I is the RMS value of phase current which determines the I^2R losses that affect the electric loading.

The magnetic loading is defined as the average air-gap flux density and can be mathematically expressed as per Equation (2):

$$B = \left(\O^{*}2P\right) / \left(\pi^{*}D_{AIR}^{*}L\right) \tag{2}$$

where P is the number of poles, L is stack length, and Ø is magnetic flux.

The supply currents to stator phases A, B, and C are given to the machine comprised of equation (3), equation (4), and equation (5) respectively as written mathematically below:

$$I_1 = I^{*}\,\mathrm{Sin}(2\pi ft + \theta) \tag{3}$$

$$I_2 = I^{*}\,\mathrm{Sin}(2\pi ft - 4\pi/3 + \theta) \tag{4}$$

$$I_3 = I^{*}\,\mathrm{Sin}(2\pi ft - 2\pi/3 + \theta) \tag{5}$$

The speed with which the sub-harmonic component of MMF rotates in the airgap is given by (6) as below.

$$n_{s(h)} = \frac{n_s}{h} = \frac{120f}{hXp} \tag{6}$$

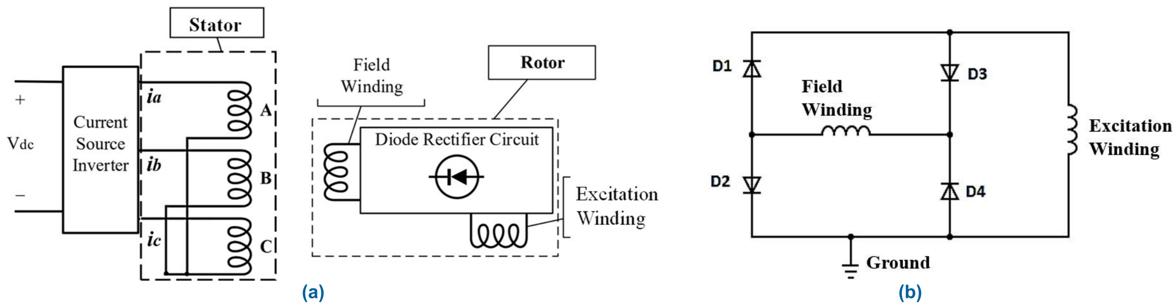

FIGURE 5. (a) Stator and rotor circuit diagram (b) Rectifier circuit to connect field winding and exciatation winding.

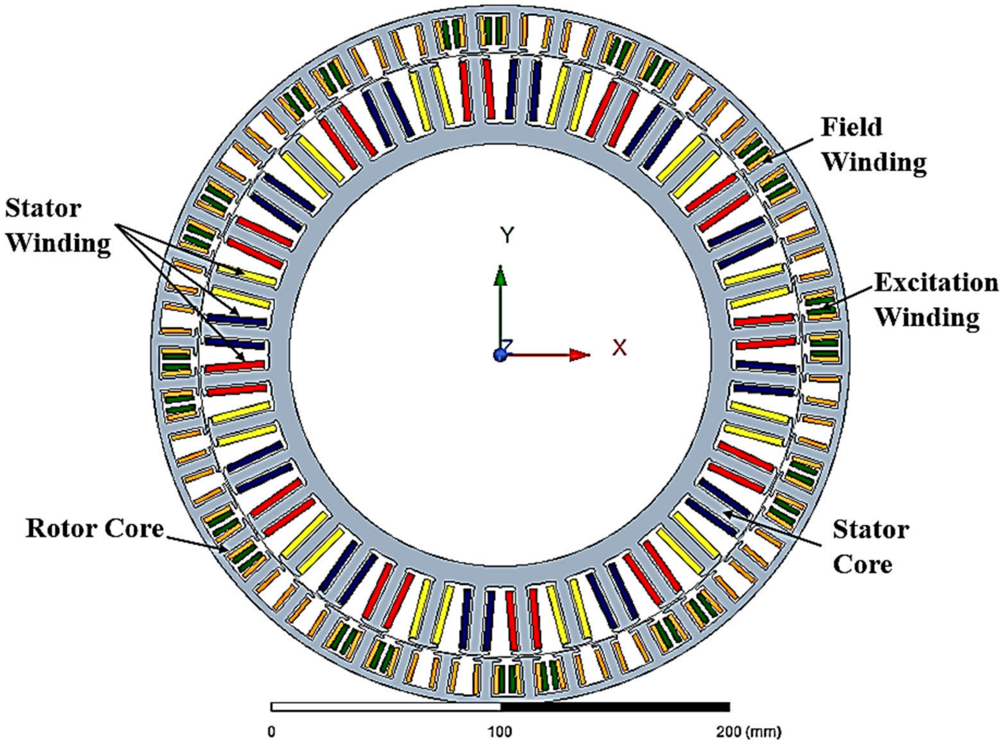

FIGURE 6. 2-D model of the proposed machine.

where $n_{s(h)}$ represents the rotating speed of the harmonic component; n_s is the fundamental synchronous speed; h is the harmonic number, f is the supplied frequency, and p is the number of poles. Taking into consideration our proposed model of 48 poles and assuming a 60 Hz frequency, the fundamental synchronous speed will be equal to 150 rpm. As we can observe the sub-harmonic component at the harmonic order of 0.5 in Fig. 4, its rotating speed will be equal to 300 rpm which is twice the speed of the fundamental component. This higher speed of rotation of the sub-harmonic component has the capability to be induced on the rotor as the rotor turns in synchronism with the fundamental component of MMF. To achieve this induction, the rotor needs to have a special winding called excitation winding. Once the voltages are induced in the excitation winding of the rotor, are rectified with the help of the rotating rectifier which is installed on the rotor. The rectified DC current is fed to the rotor field winding. The stator and rotor circuit diagram is shown in Fig. 5(a). The stator has three-phase concentrated winding fed by a 3 phase current source inverter. The rotor has two windings, field winding and excitation winding. The diode rectifier circuit is connected between the excitation winding and the field winding. The rotor circuit is shown in Fig. 5 (b).

The 2-D model employed for the proposed machine has been shown in Fig. 6 and its parameters are tabulated in Table 1. The machine has an outer rotor design where the stator is on the inner side.

The proposed machine has been employed to be used in a dual-speed application such as a washing machine. In washing machines, the washing cycle is conducted at 46 rpm while the drying cycle is conducted at 1370 rpm.

It can be noticed from Fig. 6 that the excitation winding is placed in half of the slots of the rotor only. This is because the sub-harmonic component of harmonic order 0.5 has to be induced in the excitation winding. If the stator MMF's fundamental component represents 48 poles, then the excavation

TABLE 1. Proposed machine parameters.

Parameter	Units	Values
Slots	-	36
Field Winding Poles	-	48
Harmonic Winding Poles	-	24
Stator OD/ID	mm	265.0/186.0
Rotor OD/ID	mm	308.0/267.0
Air-gap length	mm	1
Axial length	mm	24
Washing Mode Speed	rpm	46
Drying Mode Speed	rpm	1370
Frequency @ washing mode	Hz	18.4
Frequency @ drying mode	Hz	548

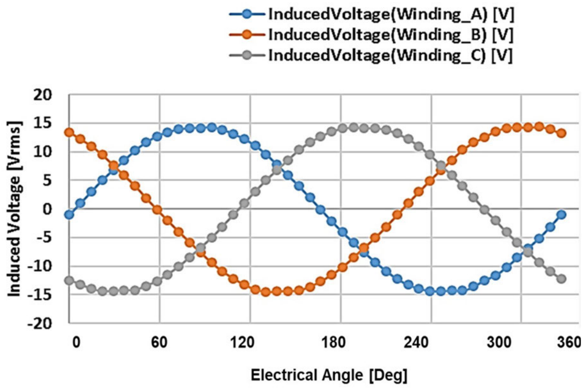

(a)

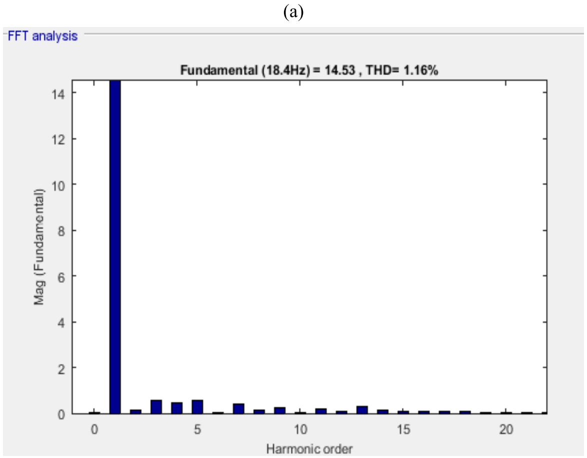

(b)

FIGURE 7. No-Load Analysis (a) Back-EMF @ 46 rpm with 5.83 A field current. (b) Harmonic Components.

winding has to be 24 poles (half of the fundamental component poles). The field winding has to be of the same pole number as that of the fundamental component of stator MMF i.e., 48 poles.

III. 2-D FINITE ELEMENT ANALYSIS

To examine the performance of the proposed machine, it has been simulated using 2-D FEA employing Ansys electromagnetic Software. Also, a conventional WRSM (C-WRSM) model without using the brushless technique was designed whose field windings are fed with the DC current directly. The input power and all other machine parameters for

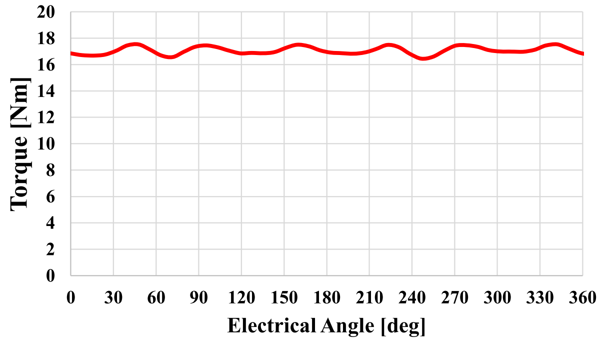

(a)

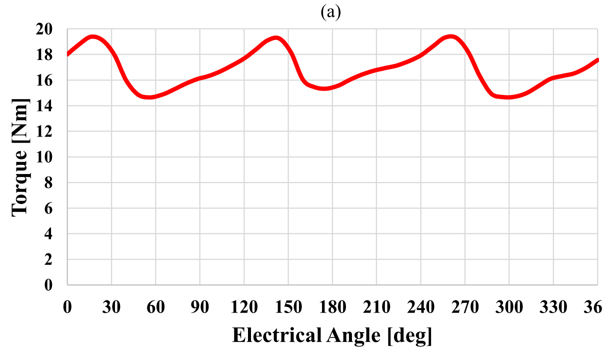

(b)

FIGURE 8. Electromagnetic torque of (a) C-WRSM @ 46rpm (b) BL-WRSM @ 46pm.

C-WRSM and the proposed BL-WRSM are kept the same for legitimate comparison.

A. NO-LOAD ANALYSIS

Firstly the WRSM is simulated in a no-load mode where only the field winding on the rotor is excited by DC current. The field current value is 5.83 A. The no-load analysis was performed at 46 rpm which is the washing mode speed. The no-load voltages are shown in Fig. 7(a) and its harmonic components are shown in Fig. 7(b). The RMS value of 10.3 V was achieved. The total harmonic distortion (THD) in the voltage was 1.16% which can be calculated using the Fig. 7(b).

B. WASHING MODE PERFORMANCE

For washing mode, the proposed machine and C-WRSM are simulated at 46 rpm. The output torque of the C-WRSM and proposed BL-WRSM are shown in Fig. 8-a and 8-b, respectively.

The average value of torque achieved in C-WRSM is 17.14 Nm with a torque ripple of 5.22%. Whereas, the average achieved in the BL-WRSM is 16.3891 Nm and a torque ripple of 25.12 %. The reason for the higher torque ripple in the proposed BL-WRSM is the pulsations in the rectified DC current provided to the field winding. Fig. 9 shows the rectified field current for BL-WRSM at 46 rpm. The flux density plot of the BL-WRSM at 46 rpm is shown in Fig. 10. The flux density of the core is less than 2 T.

C. DRYING MODE PERFORMANCE

For the drying mode both the C-WRSM and BL-WRSM are simulated at 1370 rpm.

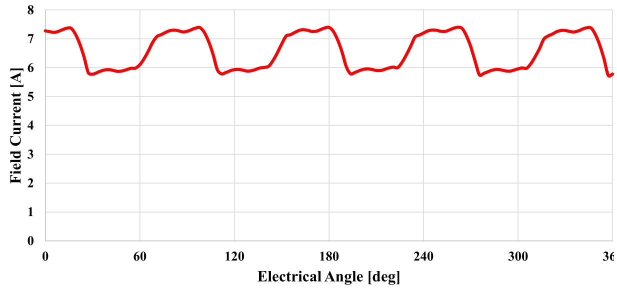

FIGURE 9. Field Current for BL-WRSM @ 46 rpm.

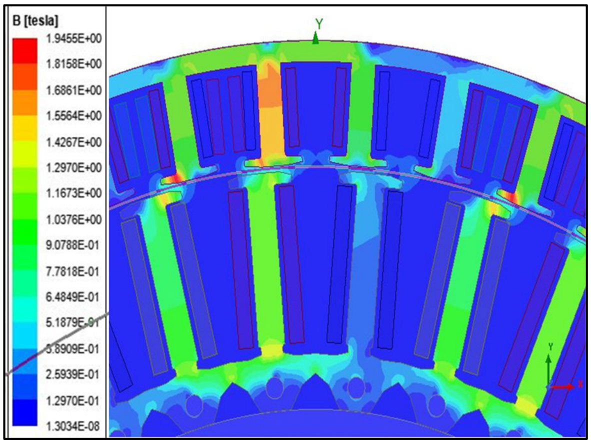

FIGURE 10. Flux Density Plot for BL-WRSM @ 46 rpm.

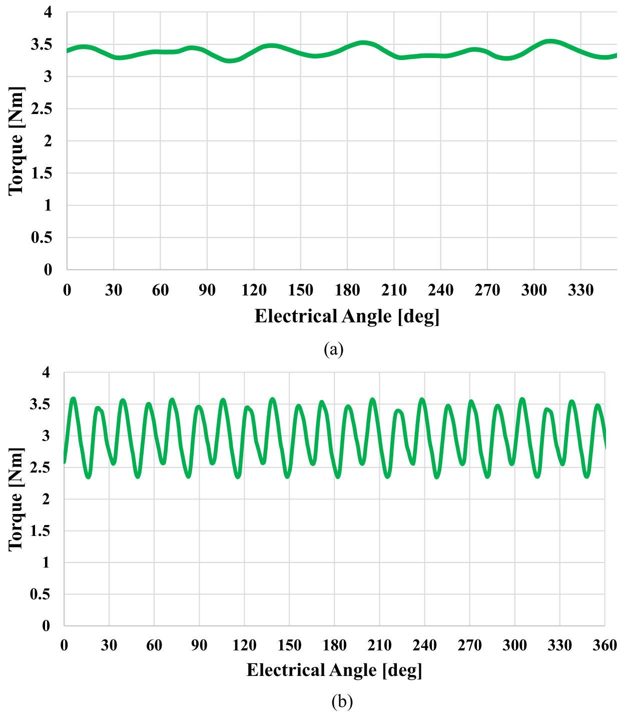

FIGURE 11. Electromagnetic torque of (a) C-WRSM @ 1370 rpm (b) BL-WRSM @ 1370rpm.

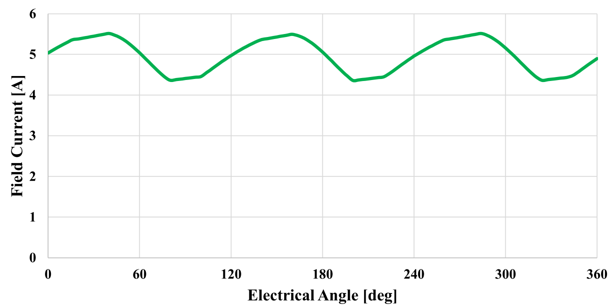

FIGURE 12. Field Current for BL-WRSM @ 1370 rpm.

The output torque of the C-WRSM and proposed BL-WRSM at drying mode is shown in Fig. 11-a and 11-b, respectively.

For the drying mode, the average value of torque achieved in C-WRSM is 3.37 Nm with a torque ripple of 8.81%. Whereas, the average achieved in the BL-WRSM is 3.03 Nm and a torque ripple of 39.7 %. Fig. 12 shows the rectified field current for BL-WRSM at 1370 rpm. The flux density plot of the BL-WRSM at 1370rpm is shown in Fig. 13. The flux density of the core is less than 2 T.

From Table 2, we can see that the proposed BL-WRSM has reduced average torque, higher torque ripple, and less efficiency compared to C-WRSM, in both modes of operation. The average torque of CWRSM for washing and drying modes is 17.14 Nm and 3.37 Nm respectively. While, for the BL-WRSM, the average torque for washing and drying modes is 16.34 Nm and 3.03 Nm. We can see that the BL-WRSM has achieved the required torque but its torque reduced from the CWRSM. The reason behind this reduction in torque is the fact that CWRSM gets rotor power from an external DC power source while the BL-WRSM's rotor does not require any external power source and rotor power is induced from the stator's MMF. Also, the rectified field current in the BL-WRSM shown in Fig. 9 and Fig. 12 has ripples while for the CWRSM, pure DC current is supplied to the rotor field current. This fact also reduces the average torque of the machine. The advantage of using the brushless topology is the avoidance of brush replacement, maintenance, and sparking. Furthermore, in future studies, optimization of BL- WRSM will be conducted to improve its performance.

For the BL-WRSM, a single-phase bridge rectifier will cost less than 5 USD. In comparison, for a CWRSM, a DC power source, brushes, and slip rings will be used. Additionally, the main disadvantage of CWRSM is the maintenance required for the brushes and slip rings which will add to the recurring cost. The cost comparison of active material is presented in table 3. The converter/drive for both, the proposed and conventional machines will almost be of the same size as there is no significant change in the input and output powers.

For the rare earth PMSM, the efficiency in washing mode (46rpm) is 47% while for the drying mode (1370rpm) is 83%. We can see that the efficiency of PMSM is better than the proposed BL-WRSM at washing mode but at drying mode,

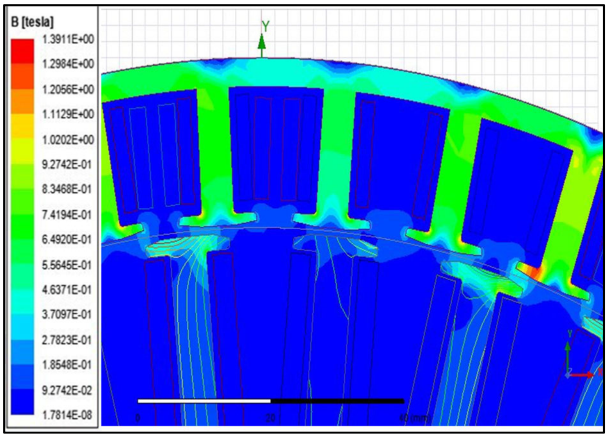

FIGURE 13. Flux Density Plot for BL-WRSM @ 1370 rpm.

TABLE 2. Performance comparison.

Parameter	Unit	CWRSM Washing Mode	CWRSM Spin Mode	BL-WRSM Washing mode	BL-WRSM Spin mode
Torque	Nm	17.14	3.37	16.34	3.03
Torque ripple	%	5.22	8.81	25.12	39.77
Harmonic winding current	A	-	-	5.7	3.63
Field finding current	A	5.83	4.16	6.26	4.87
Rotor copper loss	W	41.12	20.93	55.48	31.99
Stator copper loss	W	87.33	33.48	87.33	33.48
Efficiency	η	38.82	86.87	35.35	84.97

TABLE 3. Cost comparison of active material.

Parameter	CWRSM	BL-WRSM
Rotor Copper Used (kg)	0.209	0.31
Stator Copper Used (kg)	1.085	1.085
Total copper used (kg)	1.294	1.395
Steel laminations (kg) (rotor + stator)	3.43	3.43
Total active material (kg)	4.724	4.825
Copper Cost, USD	9.058	9.765
Lamination Cost, USD	3.43	3.43

the proposed BL-WRSM is more efficient. Also, the rare earth PMSM has a higher cost than the proposed BL-WRSM.

IV. CONCLUSION

A new brushless topology based on concentrated winding arrangement has been introduced in this paper. A 36-slot, 48-pole model was introduced. The machine was simulated for dual-speed operation at 46 rpm and 1370 rpm. The proposed topology achieved the desired torque at both speeds but its performance lags behind the C-WRSM. Nevertheless, the advantage of using such kind of machine is the avoidance of brushes that require regular maintenance, cause sparking, and create noise. In the future, this topology will be further analyzed and optimized for better performance.

REFERENCES

[1] A. H. King and R. G. Eggert, "Critical materials for permanent magnets," in *Modern Permanent Magnets*, J. Croat and J. Ormerod, Eds. Sawston, U.K.: Woodhead Publishing, 2022, ch. 10, pp. 343–370, doi: 10.1016/B978-0-323-88658-1.00003-0.

[2] Q. Ali, T. A. Lipo, and B.-I. Kwon, "Design and analysis of a novel brushless wound rotor synchronous machine," *IEEE Trans. Magn.*, vol. 51, no. 11, pp. 1–4, Nov. 2015, doi: 10.1109/TMAG.2015.2440433.

[3] S. S. H. Bukhari, Q. Ali, J. Doval-Gandoy, and J.-S. Ro, "High-efficient brushless wound rotor synchronous machine topology based on sub-harmonic field-excitation technique," *Energies*, vol. 14, no. 15, p. 4427, Jul. 2021, doi: 10.3390/en14154427.

[4] Q. Ali, S. S. H. Bukhari, and S. Atiq, "Variable-speed, sub-harmonically excited BL-WRSM avoiding unbalanced radial force," *Electr. Eng.*, vol. 101, no. 1, pp. 251–257, Apr. 2019, doi: 10.1007/s00202-019-00772-2.

[5] Q. Ali, S. Atiq, T. A. Lipo, and B.-I. Kwon, "PM assisted, brushless wound rotor synchronous machine," *J. Magn.*, vol. 21, no. 3, pp. 399–404, Sep. 2016.

[6] M. Ayub, S. Atiq, Q. Ali, A. Hussain, and B.-I. Kwon, "Dual-mode wound rotor synchronous machine for variable speed applications," *IEEE Access*, vol. 8, pp. 115812–115822, 2020, doi: 10.1109/ACCESS.2020.2999609.

[7] A. Hussain, S. Atiq, and B.-I. Kwon, "Consequent-pole hybrid brushless wound-rotor synchronous machine," *IEEE Trans. Magn.*, vol. 54, no. 11, pp. 1–5, Nov. 2018, doi: 10.1109/TMAG.2018.2837690.

[8] M. Ayub, A. Hussain, G. Jawad, and B.-I. Kwon, "Brushless operation of a wound-field synchronous machine using a novel winding scheme," *IEEE Trans. Magn.*, vol. 55, no. 6, pp. 1–4, Jun. 2019, doi: 10.1109/TMAG.2019.2893883.

[9] S. Tariq, J. Ikram, S. S. H. Bukhari, Q. Ali, A. Hussain, and J.-S. Ro, "Design and analysis of single inverter-fed brushless wound rotor Vernier machine," *IEEE Access*, vol. 10, pp. 101609–101621, 2022, doi: 10.1109/ACCESS.2022.3209501.

[10] A. Roshanzamir, K.-Y. Hwang, S.-H. Lee, J.-W. Kwon, M. Ayub, and B.-I. Kwon, "Dual-mode brushless wound rotor synchronous machine for high starting torque," *IEEE Access*, vol. 10, pp. 41657–41663, 2022, doi: 10.1109/ACCESS.2022.3167886.

[11] G. Jawad, Q. Ali, T. A. Lipo, and B.-I. Kwon, "Novel brushless wound rotor synchronous machine with zero-sequence third-harmonic field excitation," *IEEE Trans. Magn.*, vol. 52, no. 7, pp. 1–4, Jul. 2016, doi: 10.1109/TMAG.2015.2512281.

[12] L. Sun, X. Gao, F. Yao, Q. An, and T. Lipo, "A new type of harmonic current excited brushless synchronous machine based on an open winding pattern," in *Proc. IEEE Energy Convers. Congr. Expo. (ECCE)*, Pittsburgh, PA, USA, Sep. 2014, pp. 2366–2373, doi: 10.1109/ECCE.2014.6953719.

[13] D. Martinello, S. Rubino, and R. Bojoi, "An eDrive-based estimation method of the laundry unbalance and laundry inertia for washing machine applications," *Energies*, vol. 14, no. 3, p. 637, Jan. 2021, doi: 10.3390/en14030637.

[14] Statista. *Smart Appliances Revenue Worldwide 2017–2025*. Accessed: May 31, 2022. [Online]. Available: https://www.statista.com/forecasts/1221132/global-revenue-smart-appliances-market

[15] Y. Honda and Y. Takeda, "Technical evolution of permanent magnet synchronous motors for home appliances," *IEEJ Trans. Electr. Electron. Eng.*, vol. 2, no. 2, pp. 118–124, Mar. 2007, doi: 10.1002/TEE.20118.

[16] P. Yang, W. Shi, Y. Qiu, B. Li, and Y. Gan, "Enhanced efficiency of direct-drive switched reluctance motor with reconfigurable winding topology," *IEEE Access*, vol. 10, pp. 62976–62990, 2022, doi: 10.1109/ACCESS.2022.3183133.

[17] G. F. Lukman, S. Shahida, K.-I. Jeong, and J.-W. Ahn, "Characteristics analysis of a 24/16 outer-rotor switched reluctance motor with T-type stator pole for performance improvement," in *Proc. 24th Int. Conf. Electr. Mach. Syst. (ICEMS)*, Gyeongju, South Korea, Oct. 2021, pp. 355–359, doi: 10.23919/ICEMS52562.2021.9634639.

[18] P. Upadhyay and K. Ragavan, "Design of two-phase 4/6 switched reluctance motor for bidirectional starting in washing machine application," *IEEE Trans. Ind. Appl.*, vol. 59, no. 2, pp. 1519–1529, Mar. 2023, doi: 10.1109/TIA.2022.3221908.

[19] N. Baloch, J.-W. Kwon, M. Ayub, and B.-I. Kwon, "Low-cost dual-mechanical-port dual-excitation machine for washing machine application," *IEEE Access*, vol. 7, pp. 87141–87149, 2019, doi: 10.1109/ACCESS.2019.2926302.

[20] M. S. Islam, M. A. Kabir, R. Mikail, and I. Husain, "Method to minimize space harmonics of fractional slot concentrated windings in AC machines," in *Proc. IEEE Energy Convers. Congr. Expo. (ECCE)*, Portland, OR, USA, Sep. 2018, pp. 1563–1568, doi: 10.1109/ECCE.2018.8557890.

[21] H. Y. Sun and K. Wang, "Space harmonics elimination for fractional-slot windings with two-slot coil pitch," *IEEE Access*, vol. 7, pp. 106961–106972, 2019, doi: 10.1109/ACCESS.2019.2933256.

SHEERAZ AHMED was born in Shikarpur, Pakistan. He received the B.Sc. degree in electrical engineering from QUEST Nawabshah, and the M.E. degree from Sukkur IBA University. His research interest includes the design of electrical machines and controls.

MUDASSIR RAZA SIDDIQI was born in 1991. He received the B.Sc. degree in electrical engineering from the University of Engineering and Technology Taxila, Pakistan, in 2012, the M.S. degree in electrical engineering from Hanyang University, South Korea, in 2017, and the Ph.D. degree from Incheon National University, South Korea, in 2022. From 2017 to 2018, he was a Researcher with Nex-M Protohouse, Ansan, South Korea. He is currently a Research Professor with the Department of Electrical Engineering, Incheon National University. His research interest includes the design and control of electric machines.

QASIM ALI was born in Abbottabad, Pakistan, in 1989. He received the B.S. degree in electronic engineering from COMSATS University Islamabad, Abbottabad Campus, Pakistan, in 2013, and the Ph.D. degree from the Energy Conversion Systems Laboratory, Hanyang University, South Korea, in August 2018. He is currently an Assistant Professor with the Department of Electrical Engineering, Sukkur IBA University, Sindh, Pakistan. His research interest includes electric machine design and control.

TANVEER YAZDAN was born in Jampur, Punjab, Pakistan. He received the bachelor's degree in electrical engineering from the University of Engineering and Technology Taxila, Pakistan, in 2010, and M.S. leading to Ph.D. degree in electrical engineering from Hanyang University, South Korea, in 2018. From 2010 to 2013, he was an Assistant Manager with Karachi-Electric Company, Pakistan. He is currently an Assistant Professor with The University of Lahore, Pakistan. His research interest includes the design and control of electric machines.

ASIF HUSSAIN was born in Quetta, Pakistan. He received the B.Sc. degree in electrical engineering from BZU, Multan, Pakistan, in 2005, and the Ph.D. degree from the Energy Conversion Systems Laboratory, Hanyang University, South Korea, in 2018. He is currently an Assistant Professor with the Department of Electrical Engineering, University of Management and Technology, Lahore, Pakistan. His research interest includes wound rotor synchronous machine design and control.

JIN HUR (Fellow, IEEE) received the Ph.D. degree in electrical engineering from Hanyang University, Seoul, South Korea, in 1999.

From 1999 to 2000, he was with the Department of Electric Engineering, Texas A&M University, College Station, TX, USA, as a Postdoctoral Research Associate. From 2000 to 2001, he was a Research Professor of electrical engineering for BK21 projects with Hanyang University. From 2002 to 2007, he was the Director of the Intelligent Mechatronics Research Center, Korea Electronics Technology Institute (KETI), Puchon, South Korea, where he was involved on the development of special electric machines and systems. From 2008 to August 2015, he was an Associate Professor with the School of Electric Engineering, University of Ulsan, Ulsan, South Korea. Since August 2015, he has been a Professor with the Department of Electrical Engineering, Incheon National University, Incheon, South Korea. He has authored and coauthored over 140 publications on electric machine design, analysis and control, and power electronics. He has one pending U.S. patent and 20 pending Korean patents. His current research interests include high-performance electrical machines, modeling, drives, new concept actuators for special purposes, and numerical analysis of electromagnetic fields.

Dr. Hur is an Associate Editor of IEEE Transactions on Power Electronics.